

## High efficiency Raman memory by suppressing radiation trapping

This content has been downloaded from IOPscience. Please scroll down to see the full text.

2017 New J. Phys. 19 063034

(<http://iopscience.iop.org/1367-2630/19/6/063034>)

View [the table of contents for this issue](#), or go to the [journal homepage](#) for more

Download details:

IP Address: 192.76.8.93

This content was downloaded on 15/08/2017 at 11:29

Please note that [terms and conditions apply](#).

You may also be interested in:

[Optical quantum memory based on electromagnetically induced transparency](#)

Lijun Ma, Oliver Slattery and Xiao Tang

[Interfacing GHz-bandwidth heralded single photons with a warm vapour Raman memory](#)

P S Michelberger, T F M Champion, M R Sprague et al.

[High-fidelity polarization storage in a gigahertz bandwidth quantum memory](#)

D G England, P S Michelberger, T F M Champion et al.

[Storage and manipulation of light using a Raman gradient-echo process](#)

M Hosseini, B M Sparkes, G T Campbell et al.

[Two-way interconversion of millimeter-wave and optical fields in Rydberg gases](#)

Martin Kiffner, Amir Feizpour, Krzysztof T Kaczmarek et al.

[Electromagnetically induced transparency and four-wave mixing in a cold atomic ensemble with large optical depth](#)

J Geng, G T Campbell, J Bernu et al.

[Efficient light storage with reduced energy loss via nonlinear compensation in rubidium vapor](#)

Gang Wang, Wei Zhou, Hong-Li Chen et al.

[Efficient optical pumping and high optical depth in a hollow-core photonic-crystal fibre for a broadband quantum memory](#)

Michael R Sprague, Duncan G England, Amir Abdolvand et al.

[Interplay of classical and quantum dynamics in a thermal ensemble of atoms](#)

Arif Warsi Laskar, Niharika Singh, Arunabh Mukherjee et al.



## PAPER

## High efficiency Raman memory by suppressing radiation trapping

S E Thomas<sup>1,2</sup>, J H D Munns<sup>1,2</sup>, K T Kaczmarek<sup>1</sup>, C Qiu<sup>1,3</sup>, B Brecht<sup>1</sup>, A Feizpour<sup>1</sup>, P M Ledingham<sup>1</sup>,  
I A Walmsley<sup>1</sup>, J Nunn<sup>1</sup> and D J Saunders<sup>1</sup><sup>1</sup> Clarendon Laboratory, University of Oxford, Parks Road, Oxford OX1 3PU, United Kingdom<sup>2</sup> QOLS, Blackett Laboratory, Imperial College London, London SW7 2BW, United Kingdom<sup>3</sup> Department of Physics, Quantum Institute for Light and Atoms, State Key Laboratory of Precision Spectroscopy, East China Normal University, Shanghai 200062, People's Republic of ChinaE-mail: [sarah.thomas@physics.ox.ac.uk](mailto:sarah.thomas@physics.ox.ac.uk)**Keywords:** quantum memory, radiation trapping, atomic vapour, quenchingSupplementary material for this article is available [online](#)RECEIVED  
2 February 2017REVISED  
5 May 2017ACCEPTED FOR PUBLICATION  
26 May 2017PUBLISHED  
3 July 2017Original content from this  
work may be used under  
the terms of the [Creative  
Commons Attribution 3.0  
licence](#).Any further distribution of  
this work must maintain  
attribution to the  
author(s) and the title of  
the work, journal citation  
and DOI.

## Abstract

Raman interactions in alkali vapours are used in applications such as atomic clocks, optical signal processing, generation of squeezed light and Raman quantum memories for temporal multiplexing. To achieve a strong interaction the alkali ensemble needs both a large optical depth and a high level of spin-polarisation. We implement a technique known as quenching using a molecular buffer gas which allows near-perfect spin-polarisation of over 99.5% in caesium vapour at high optical depths of up to  $\sim 2 \times 10^5$ ; a factor of 4 higher than can be achieved without quenching. We use this system to explore efficient light storage with high gain in a GHz bandwidth Raman memory.

## 1. Introduction

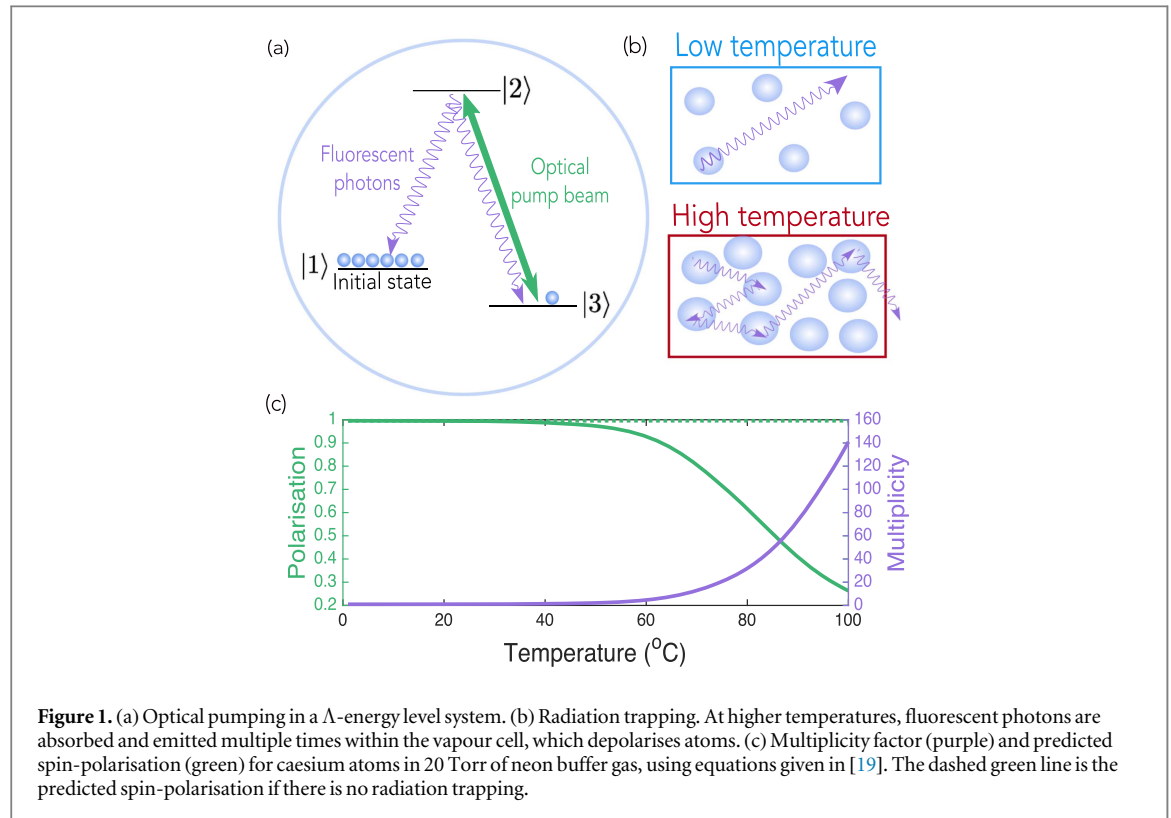
Raman scattering in alkali vapours provides an optical interface with atomic spins. Optically dense alkali vapours can serve as a frequency reference for atomic clocks and magnetometry [1, 2], a buffer in optical signal processing [3], and in the quantum domain, provide a source of squeezed light via four-wave mixing (FWM) [4, 5] or a medium for storing and synchronising photons, via the Raman- and DLCZ-type quantum memory protocols [6–15]. In each of these examples, the desired light-matter coupling is a collective effect, where the coupling strength scales favourably with the optical depth  $d$ , which is proportional to the atomic density.

Very high atomic densities can be achieved without complex atom trapping by heating a vapour cell, but in vapour cell systems the ability to spin-polarise the ensemble by optical pumping [16] is hampered by radiation trapping at high densities [17]. This problem is greatly mitigated in hollow waveguides, where there is only high optical depth in one dimension, but here high densities are challenging due to surface adsorption [18]. Here we show that introducing a molecular buffer gas into a vapour cell suppresses radiation trapping via collisional quenching and enables high quality spin-polarisation even at high temperatures. We use this system to demonstrate efficient light storage with very high and controllable gain, and these results demonstrate a route towards high efficiency storage of non-classical light.

## 2. Optical pumping in alkali vapours

To enable strong Raman interactions, a high-density atomic ensemble needs to be prepared in a single ground state via optical pumping [16]. To initialise the ensemble in the ground state  $|1\rangle$  (defined in figure 1(a)), a strong pump beam resonant with the  $|3\rangle \leftrightarrow |2\rangle$  transition illuminates the ensemble. This excites atoms out of state  $|3\rangle$ , which then decay via fluorescence back to the ground states. Atoms in  $|3\rangle$  are continuously depleted and the atoms all accumulate in  $|1\rangle$  after several cycles of excitation and decay.

However, when an atom decays down to one of the ground states by fluorescence, it emits a photon. Thus a background population of photons resonant with  $|1\rangle \leftrightarrow |2\rangle$  transition is established. This radiation can transfer an electron from  $|1\rangle$  to  $|2\rangle$ , which can then decay to  $|3\rangle$ —the reverse of optical pumping. If the alkali



vapour is optically thick these photons can be absorbed and re-emitted multiple times, and ‘un-pump’ many atoms in the vapour (see figure 1(b)). This effect is known as radiation trapping and limits the spin-polarisation that can be achieved when the vapour has a sufficiently high optical depth in multiple dimensions [17].

The effect that radiation trapping has on optical pumping of alkali vapours is characterised using the multiplicity factor  $M$ , which is the average number of times a photon is re-absorbed and emitted before it leaves the vapour. It can be shown that  $M$  increases exponentially in the number density of the vapour, which itself is exponential in temperature, and in a cylindrical bulk vapour cell  $M$  can exceed 100 for typical operational conditions [19], as shown in figure 1(c).

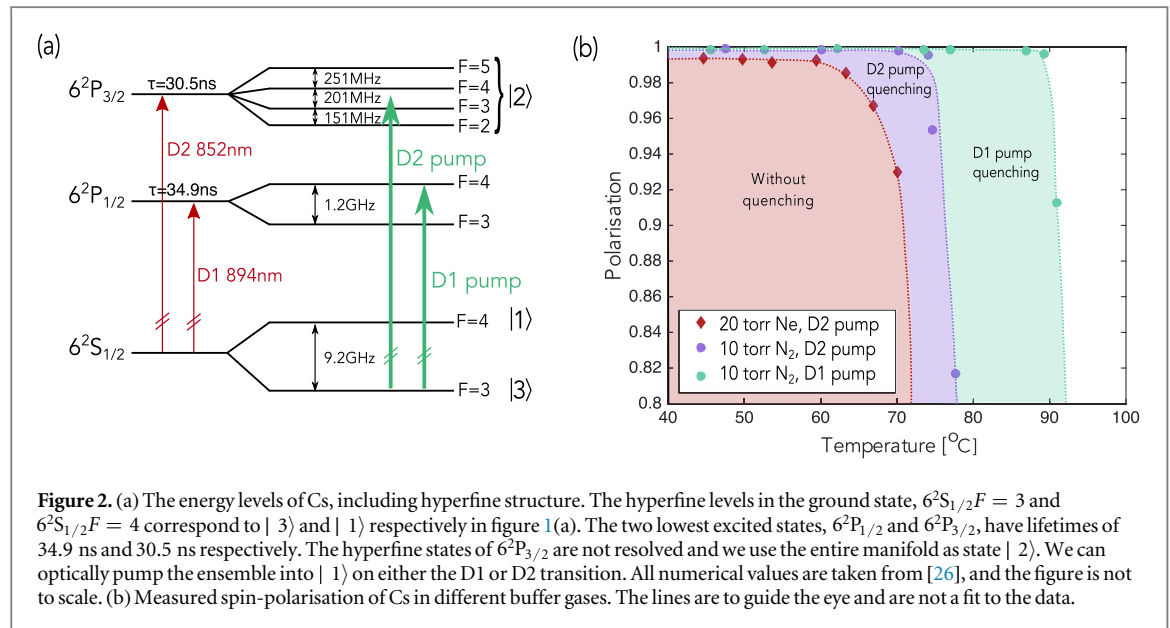
In alkali vapour systems, a buffer gas is often added to the vapour to inhibit diffusion of the alkali atoms, and the choice of the species and pressure of the buffer gas plays a vital role in many experiments. To ensure high spin-polarisation, it is crucial that the collisions between the alkali atoms and the buffer gas are spin-preserving and induce very low rates of population transfer between the ground states. The spin-relaxation rate of polarised alkali vapours in different buffer gases has been studied, and is found to be low in inert gases such as the noble gases and molecular nitrogen [20]. Another important consideration for the choice of buffer gas is the relative trade-off between the diffusion rate versus the induced pressure broadening. In this work, we choose a buffer gas which also enables a non-radiative energy transfer pathway from atoms in the excited state  $|2\rangle$  to the buffer gas via collisional quenching.

Our group previously used 20 Torr of neon as a buffer gas for Raman memory experiments as neon is spin-preserving and provides an appropriate trade-off between atomic diffusion and pressure broadening for our previous quantum memory experiments [14, 21]. Figure 1(c) shows the numerical values for the multiplicity as a function of temperature for caesium (Cs) vapour with this choice of buffer gas. We can see that the radiation trapping effect becomes significant for  $T \gtrsim 70^\circ\text{C}$ , and this dramatically reduces the spin-polarisation at high temperatures. Here we investigate optical pumping in Cs vapour in an alternative buffer gas. If we can reduce radiation trapping and achieve high spin-polarisation at high temperatures, then we can increase the Raman interaction strength by operating at higher optical depths.

To suppress radiation trapping we introduce a mechanism whereby atoms decay from the excited state without fluorescence resonant with the  $|1\rangle \leftrightarrow |2\rangle$  transition. If a molecular buffer gas is introduced which has an optical transition close in energy to the atomic transition, alkali atoms in the excited state collide with the molecules and transfer their energy to the molecule. The buffer gas molecules in their excited vibrational state can then decay via a phonon sideband, thereby relaxing to the ground state without emitting photons resonant with the optical alkali transitions. This reduces the number of resonant fluorescent photons produced in the optical pumping process and therefore suppresses radiation trapping, in a process known as collisional

**Table 1.** The diffusion constants and pressure broadening coefficients for the two buffer gases considered. The diffusion parameters are extracted experimentally using the method presented in [24], and the errors denote 95% confidence bounds. The pressure broadening coefficients are at a temperature of 313 K quoted from [25].

Species	$D_0$ (cm <sup>2</sup> s <sup>-1</sup> )	$\gamma$ (MHz Torr <sup>-1</sup> )
N <sub>2</sub>	$0.24 \pm 0.09$	$19.18 \pm 0.06$
Ne	$0.35 \pm 0.05$	$9.81 \pm 0.06$



quenching. Quenching by introduction of a molecular buffer gas is a common technique used to limit radiation trapping, for example in spin-exchange optical pumping [22]. Quenching has been used previously in studies of electromagnetically induced transparency storage [23], however this is the first time, to our knowledge, that it has been applied in the context of off-resonant light storage techniques.

To investigate the effect of collisional quenching, we compare the spin-polarisation of Cs vapour with two different buffer gases: neon (Ne) and molecular nitrogen (N<sub>2</sub>). The latter gas provides a pathway for quenching as vibrational transitions exist which are very close in energy to the optical transitions of Cs [16].

We first measured the diffusion of Cs in the two buffer gases using the method described in [24] (see supplementary material available online at [stacks.iop.org/NJP/19/063034/mmedia](https://stacks.iop.org/NJP/19/063034/mmedia)). The results are given in table 1, and we find that the diffusion of Cs in N<sub>2</sub> is slower than in Ne at the same buffer gas pressure, and therefore for the case of a Raman memory, it is a viable buffer gas to ensure sufficient Raman interaction times for light storage on timescales  $\sim 1$   $\mu$ s. The pressure broadening of the Cs transitions is twice as high in N<sub>2</sub> buffer gas compared to Ne (table 1) and hence to ensure a fair comparison we investigate spin-polarisation in 20 Torr of Ne and with 10 Torr of N<sub>2</sub>.

The spin-polarisation of Cs vapour as a function of temperature is shown in figure 2(b). A description of how the spin-polarisation of a vapour is measured is given in the supplementary material. We see high spin-polarisation of the ensemble at low temperatures in all buffer gases, and then a sharp decline with increasing temperature which is due to radiation trapping. However, for temperatures above 70 °C, the spin-polarisation is significantly higher in N<sub>2</sub> than in Ne due to the reduced radiation trapping in the molecular buffer gas. This demonstrates that collisional quenching is an effective way to enable spin-polarisation at very high temperatures in this system.

We investigated optical pumping in N<sub>2</sub> buffer gas on different atomic transitions in Cs (the energy level structure is shown in figure 2(a)). The quenching cross-section, which quantifies the probability of a quenching collision occurring, is  $\sigma_Q = 77$  Å<sup>2</sup> for the D1 line and  $\sigma_Q = 69$  Å<sup>2</sup> for the D2 line [27]. Furthermore, the D1 excited state has a longer lifetime (34.9 ns compared to 30.5 ns) and therefore there is more time for a collision to occur while the atom is in the excited state. Quenching is therefore more efficient on the D1 transition as the rate of collisional quenching is higher.

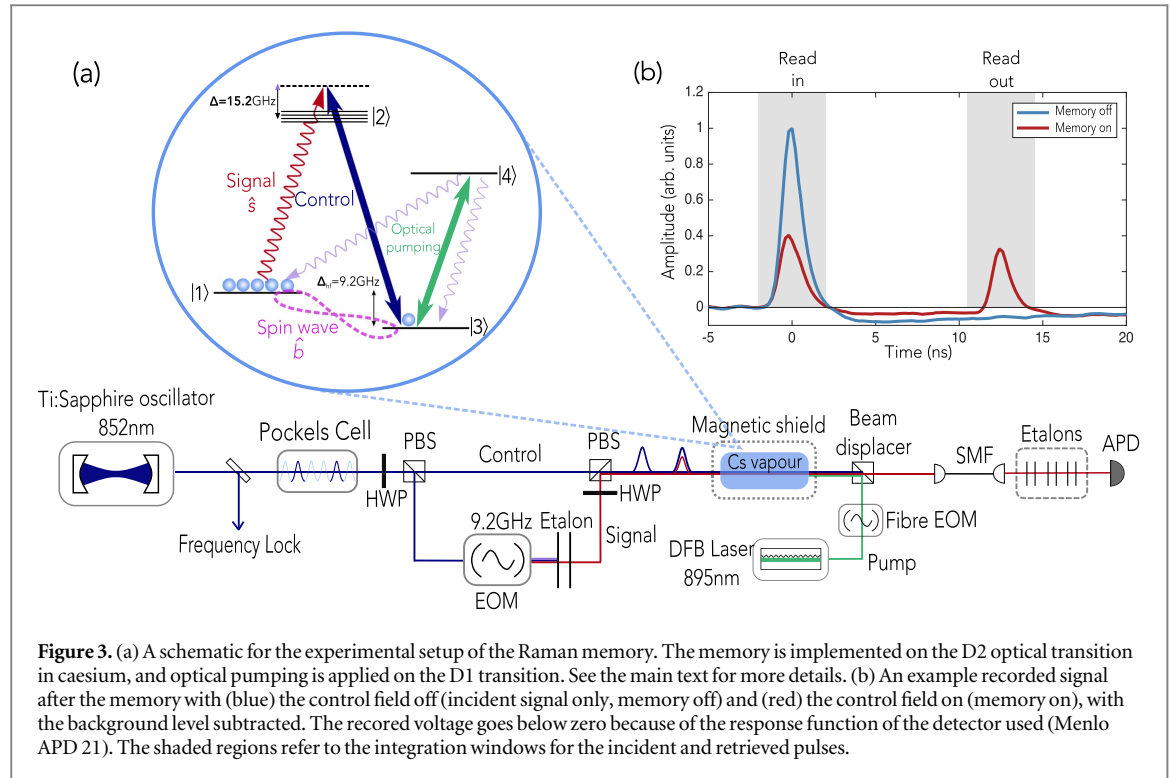


**Figure 3.** (a) A schematic for the experimental setup of the Raman memory. The memory is implemented on the D2 optical transition in caesium, and optical pumping is applied on the D1 transition. See the main text for more details. (b) An example recorded signal after the memory with (blue) the control field off (incident signal only, memory off) and (red) the control field on (memory on), with the background level subtracted. The recorded voltage goes below zero because of the response function of the detector used (Menlo APD 21). The shaded regions refer to the integration windows for the incident and retrieved pulses.

Figure 2(b) shows significantly higher spin-polarisation at temperatures above 75 °C when the optical pumping light is tuned to the D1 atomic transition due to more efficient quenching. With 10 Torr of  $N_2$  and by optically pumping on the D1 line we can now achieve spin-polarisations of over 99.5% up to 90 °C. Finally, we extract from our spin-polarisation measurements the optical depth,  $d$ , of the Cs vapour. Increasing the temperature from 70 °C to 90 °C equates to an increase of  $d$  from  $5 \times 10^4$  to  $2 \times 10^5$ . This increase of a factor of 4 is shown to significantly enhance Raman interactions, as we investigate below in the context of light storage in a Raman memory.

### 3. Raman memory

The Raman memory protocol uses a  $\Lambda$ -level scheme to adiabatically transfer population between two ground states via an off-resonant stimulated Raman transition. We implement the memory in an ensemble of Cs atoms in the vapour phase, where the hyperfine states  $6^2S_{1/2} F=3$  and  $F=4$  act as the storage state  $|3\rangle$  and initial state  $|1\rangle$ , separated by  $\Delta_{\text{hf}} = 9.2 \text{ GHz}$ , and the hyperfine manifold  $6^2P_{3/2}$  is the excited state  $|2\rangle$ , as shown in figure 3(a) [21]. The first step of the memory protocol is to spin-polarise the ensemble into the  $F=4$  ground state,  $|1\rangle$ . Imperfect spin-polarisation decreases the memory efficiency due to the lower optical depth of the memory interaction optical transition which reduces the Raman interaction strength, and can also lead to adverse noise processes, such as spontaneous Raman noise, that will decrease the fidelity of the memory operation [15]. In this work, we implement optical pumping on the D1 transition, with the  $6^2P_{1/2}$  hyperfine manifold as excited state  $|4\rangle$ , and use a buffer gas of 10 Torr of  $N_2$ , as we found above that this enabled the best spin-polarisation at high temperatures.

The Raman memory interaction is mediated by a strong control pulse which drives a two-photon Raman transition from  $|1\rangle \rightarrow |3\rangle$ . This adiabatically maps the signal mode  $\hat{s}$  onto an excitation of the ground-state coherence of the ensemble, or spin-wave mode,  $\hat{b}$ . The interaction is described by a beam-splitter Hamiltonian

$$\mathcal{H}_s \propto C_s \hat{s} \hat{b}^\dagger + \text{h.c.}, \quad (1)$$

with the coupling constant  $C_s \propto \sqrt{d\gamma\Omega}/\Delta$ , where  $d$  is the resonant optical depth and  $\gamma$  is the linewidth of the  $|1\rangle \leftrightarrow |2\rangle$  transition,  $\Omega$  is the control field Rabi frequency,  $\delta$  is the control field bandwidth,  $\Delta$  is the detuning from two-photon resonance [28], and h.c. is the Hermitian conjugate. The signal is read out of the memory by applying a second control pulse which drives the reverse process, and this is a second beam splitter interaction with the same coupling strength  $C_s$ . The total memory efficiency  $\eta_{\text{mem}}$  is proportional to  $C_s^4$ , and hence scales with the square of the optical depth,  $d$ . Memory efficiencies of 21% for single photon input states and 29% for coherent states have been achieved with GHz bandwidths and  $\mu\text{s}$  storage times [14]. In this previous work, a buffer gas of 20 Torr of Ne was used, and the Cs vapour temperature was 70 °C.

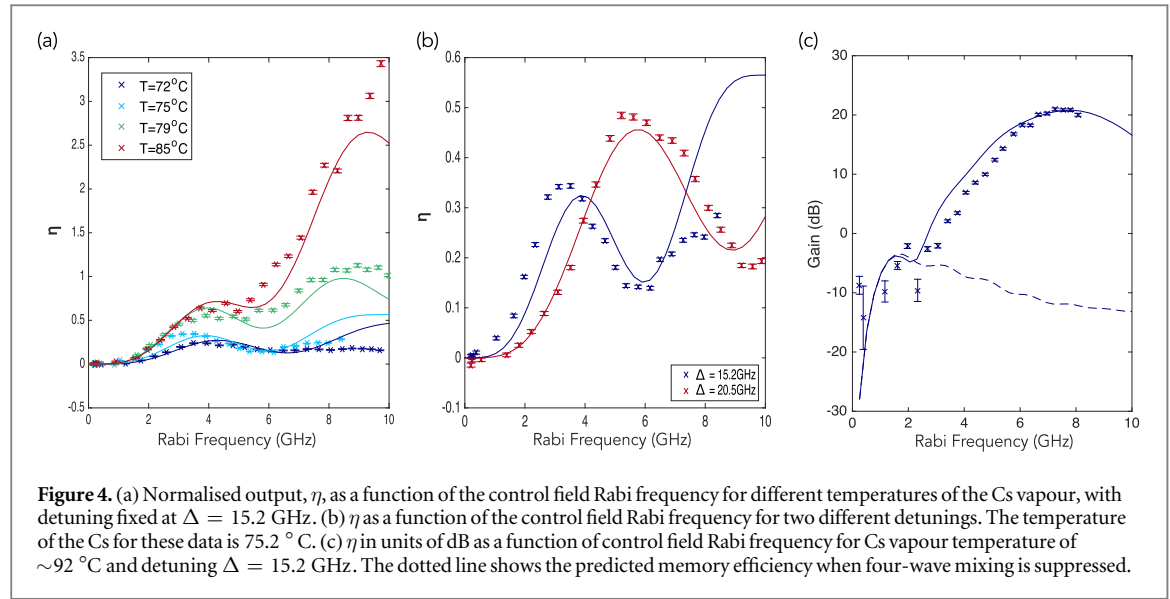


**Figure 4.** (a) Normalised output,  $\eta$ , as a function of the control field Rabi frequency for different temperatures of the Cs vapour, with detuning fixed at  $\Delta = 15.2$  GHz. (b)  $\eta$  as a function of the control field Rabi frequency for two different detunings. The temperature of the Cs for these data is  $75.2^\circ\text{C}$ . (c)  $\eta$  in units of dB as a function of control field Rabi frequency for Cs vapour temperature of  $\sim 92^\circ\text{C}$  and detuning  $\Delta = 15.2$  GHz. The dotted line shows the predicted memory efficiency when four-wave mixing is suppressed.

As well as the beam splitter interaction, this system also supports FWM due to the control field coupling to state  $|1\rangle$  and driving spontaneous anti-Stokes scattering. This interaction is described by a two-mode-squeezing Hamiltonian

$$\mathcal{H}_a \propto C_a \hat{a} \hat{b} + \text{h.c.}, \quad (2)$$

which produces excitations in both the anti-Stokes mode,  $\hat{a}$ , and the spin-wave,  $\hat{b}$ , followed by the beam-splitter Hamiltonian. The anti-Stokes coupling constant is given by  $C_a = C_s \Delta / \Delta_a$ , where the detuning of this interaction is  $\Delta_a = \Delta + \Delta_{\text{hf}}$ . In the far-off-resonant limit,  $\Delta \gg \Delta_{\text{hf}}$ , the magnitudes of the coupling strengths  $C_s$  and  $C_a$  are comparable. FWM introduces gain into the system and can significantly enhance the amplitude of the retrieved pulse. Gain is always accompanied by noise [29] and we recently showed how this noise degrades the quantum features of single photons [14], and how this can be suppressed for quantum light storage by operating the memory inside a low-finesse cavity [15]. However, operating the memory inside a cavity is much more complex experimentally and we use a non-cavity memory system as a test bed for investigating the high coupling regime, even though it is not suitable for single-photon storage.

We used the same memory setup as in previous demonstrations of the Raman memory [14] but with a higher operation temperature of up to  $92^\circ\text{C}$ , which should enable significantly higher Raman interactions. The control and signal field pulses are both derived from a mode-locked, frequency-stabilised pulsed Titanium-Sapphire (Ti:Sa) laser which generates pulses with a central wavelength of  $\sim 852$  nm and a spectral bandwidth of 1.2 GHz at a repetition rate of 80 MHz. Its exact central frequency is locked to be 15.2 GHz blue-detuned from the  $6^2\text{S}_{1/2}$  ( $F = 3$ )  $\rightarrow 6^2\text{P}_{3/2}$  transition. A Pockels cell is used to select the read-in and read-out pulses from this pulse train with a controllable separation time. The extinction ratio of the picked pulses after coupling into a single-mode fibre is approximately 40 000:1. The beam is separated on a polarising beam splitter and one arm passes through an electro-optic modulator which is modulated at a frequency of 9.2 GHz to generate sidebands at  $\pm 9.2$  GHz, one of which is used as the input signal for the memory. An etalon is used to filter the carrier frequency and the blue sideband leaving only the red modulated sideband at the required signal frequency. The input coherent state amplitude is  $|\alpha|^2 \sim 10^5$ . The signal and control fields are overlapped spatially and temporally and focused to a beam waist of  $140\mu\text{m}$  at the centre of a vapour cell. The vapour cell is inside a  $\mu$ -metal shield to reduce the residual magnetic field by a factor of  $\sim 10^3$  and limit the dephasing of the ground-state coherence.

To characterise the performance of the memory system, we normalise the retrieved signal to the input state, and define the normalised output,  $\eta$ , as the ratio of the pulse energy of the retrieved pulse and the input pulse. For the case of a noise-free memory, this quantity is simply the storage efficiency of the memory protocol,  $\eta_{\text{mem}}$ . However, in the presence of FWM this quantity represents contributions from both parts of the Hamiltonian,  $\mathcal{H}_s$  (the storage interaction) and  $\mathcal{H}_a$  (FWM gain), and hence can be larger than one. We measured  $\eta$  as a function of the control field Rabi frequency for different temperatures of the Cs ensemble, as shown in figure 4(a). For small control Rabi frequencies  $\eta$  increases quadratically with  $\Omega$ , since the Raman coupling strength  $C_s$  is proportional to  $\sqrt{d} \frac{\Omega}{\Delta}$ . However, as  $\Omega$  increases, the strong control field induces an AC Stark shift between states  $|2\rangle$  and  $|3\rangle$ , which perturbs the two-photon resonance condition and reduces the memory efficiency [28]. For each temperature this occurs at  $\Omega \approx 4$  GHz for  $\Delta = 15.2$  GHz, where the AC Stark shift becomes comparable to the spectral bandwidth of the pulse, and we see a decrease in  $\eta$  at this point. One approach to solving this



problem is to appropriately chirp the control field or signal field to remain on two-photon resonance [28], but this requires active modulation since the Stark shift is time-varying. Nevertheless, at even higher Rabi frequencies we see that  $\eta$  increases dramatically, even above 100%, due to the FWM gain process. The average number of anti-Stokes photons produced is proportional to  $\sinh^2(C_a/\delta)$ , and therefore at high control field Rabi frequency, the FWM process increases approximately exponentially in  $\Omega$  and this gain interaction dominates and amplifies the input signal. We can see in figure 4(a) that  $\eta$  is significantly greater at higher temperatures. This increase is a direct consequence of the higher Raman coupling strength due to increased optical depth which was enabled by improving the spin-polarisation at higher temperatures.

We investigated operating the Raman memory further from resonance to reduce linear absorption of the signal and decrease the AC Stark shift, as shown in figure 4(b). The Raman interaction strength is proportional to  $1/\Delta^2$  and therefore for small Rabi frequencies we see a higher efficiency when the detuning from resonance is smaller. However, the AC Stark shift  $\Delta E$  is proportional to  $\Omega^2/\Delta$ , and therefore  $\eta$  reaches higher values when we operate further from resonance due to the suppression of the AC Stark shift. This shows an additional benefit of the increased Raman interaction strength: the increase in optical depth means that we can operate further from resonance while still maintaining strong Raman coupling and therefore mitigate the AC Stark effect and achieve higher memory efficiency.

To model these data we numerically solve the linearised Maxwell–Bloch equations in one dimension in the adiabatic limit [14]. This model assumes that the excited state can be adiabatically eliminated and that the population of the states remains constant throughout the interaction, as the size of the signal field is much smaller than the number of atoms in the ensemble. The adiabatic approximation is valid when the Rabi frequency,  $\Omega$ , and the bandwidth of the signal pulse,  $\delta$ , are both significantly less than the detuning  $\Delta$ . This theory has been used to model the Raman memory previously [30], but here we test it for the first time in a regime of high optical depth and high Rabi frequency. Figure 4 shows that the model qualitatively captures the trends of the data for all temperatures, including the rollover in efficiency due to the AC Stark shift, and the continued increase at higher Rabi frequencies due to FWM gain. We therefore have confidence that this linearised model can be extended to this high coupling regime. The discrepancies at very high Rabi frequencies reflect that the adiabatic approximation is no longer valid, and we see that this approximation breaks down when  $\Omega \gtrsim \Delta/2$ . In figure 4(b) the model agrees well with the data until  $\Omega \sim 7$  GHz for a detuning of  $\Delta = 15.2$  GHz, and until  $\Omega \sim 9$  GHz for  $\Delta = 20.5$  GHz, consistent with the conclusion of a breakdown of adiabaticity at very high Rabi frequencies. The model can therefore be used to predict performance in the Raman memory at high temperatures, provided that  $\Omega \lesssim \Delta/2$ .

The data in figure 4(c) show the memory performance when the ensemble temperature is 92 °C, and the normalised output,  $\eta$ , increases up to  $\gtrsim 120$ . This demonstrates extremely strong amplification of the input signal of over 20 dB due to the strong Raman interaction. This technique therefore has potential applications as an amplified delay-line for optical signals in a room temperature system for optical signal processing applications. These results could also be applied to the generation of strongly-squeezed light via FWM in alkali vapours [5]. Adding a molecular buffer gas to increase the optical depth of a spin-polarised alkali vapour could enhance the Raman interaction strength and enable even higher two-mode squeezing.

Furthermore, these results can be applied to a cavity-enhanced Raman memory protocol where FWM noise can be effectively suppressed to allow low-noise storage of single photons [15, 31]. The dashed line in figure 4(c) shows the predicted memory efficiency if there is no FWM, and this gives an indication of the potential performance of this memory for quantum-level storage. We predict that the memory efficiency in the cavity-enhanced Raman memory presented in [15] (using the theory presented there) would increase from 9.5% to 18.8% with the addition of a molecular buffer gas because we could operate at 90 °C compared to 70 °C in the previous experiment. Therefore the strong Raman coupling enabled by collisional quenching enhances the memory interaction strength and opens the route to achieving high-efficiency storage of single photons in the near future.

## Acknowledgments

This work was supported by the UK Engineering and Physical Sciences Research Council through Standard Grant No. EP/J000051/1, Programme Grant No. EP/K034480/1, and the EPSRC NQIT Quantum Technology Hub. We acknowledge support from the Air Force Office of Scientific Research: European Office of Aerospace Research and Development (AFOSR EOARD Grant No. FA8655-09-1-3020). JN acknowledges a Royal Society University Research Fellowship, and DJS acknowledges an EU Marie-Curie Fellowship No. PIIF-GA-2013-629229. PML acknowledges a European Union Horizon 2020 Research and Innovation Framework Programme Marie Curie individual fellowship, Grant Agreement No. 705278, and BB acknowledges an H2020 Future and Emerging Technologies Grant QCUMBER (Grant Award number 665148). IAW acknowledges an ERC

Advanced Grant (MOQUACINO). CQ was supported by the China Scholarship Council (CSC Grant No. 201406140039). SET and JHDM are supported by EPSRC via the Controlled Quantum Dynamics CDT under Grants EP/G037043/1 and EP/L016524/1.

## Author contributions

This experiment was conceived and designed by DJS, and was performed by SET with assistance from DJS, PML, BB, CQ and AF. The optical pumping data were analysed by SET with assistance from JHDM. The diffusion measurements were performed by JHDM and KTK and analysed by JHDM. The Raman memory data was modelled theoretically by JN. This project was supervised by DJS, JN and IAW.

## Competing financial interests

The authors declare no competing financial interests.

## References

- [1] Hinkley N, Sherman J A, Phillips N B, Schioppo M, Lemke N D, Beloy K, Pizzocaro M, Oates C W and Ludlow A D 2013 An atomic clock with  $10^{-18}$  instability *Science* **341** 1215–8
- [2] Budker D and Romalis M 2007 Optical magnetometry *Nat. Phys.* **3** 227–34
- [3] Tucker R S, Ku P S and Chang-Hasnain C J 2005 Slow-light optical buffers: capabilities and fundamental limitations *J. Lightwave Technol.* **23** 4046
- [4] Boyer V, Marino A M, Pooser R C and Lett P D 2009 Entangling light in its spatial degrees of freedom with four-wave mixing in an atomic vapor *ChemPhysChem* **10** 755–60
- [5] McCormick C F, Marino A M, Boyer V, Jones K M and Lett P D 2008 Strong low-frequency quantum correlations from a four-wave mixing amplifier *Phys. Rev. A* **78** 043816
- [6] Lvovsky A I et al 2009 Optical quantum memory *Nat. Photon.* **3** 706–14
- [7] Duan L-M, Lukin M D, Cirac J I and Zoller P 2001 Long-distance quantum communication with atomic ensembles and linear optics *Nature* **414** 413–8
- [8] Gorshkov A V, Andre A, Fleischhauer M, Sorensen A S and Lukin M D 2007 Universal approach to optimal photon storage in atomic media *Phys. Rev. Lett.* **98** 123601
- [9] Novikova I, Phillips N B and Gorshkov A V 2008 Optimal light storage with full pulse-shape control *Phys. Rev. A* **78** 021802
- [10] Phillips N B, Gorshkov A V and Novikova I 2008 Optimal light storage in atomic vapor *Phys. Rev. A* **78** 023801
- [11] Hosseini M, Sparkes B M, Campbell G, Lam P K and Buchler B C 2011 High efficiency coherent optical memory with warm rubidium vapour *Nat. Commun.* **2** 174
- [12] Hosseini M, Campbell G, Sparkes B M, Lam P K and Buchler B C 2011 Unconditional room-temperature quantum memory *Nat. Phys.* **7** 794–8
- [13] Namazi M, Kupchak C, Jordaan B, Shahrokshahi R and Figueroa E 2015 Unconditional polarization qubit quantum memory at room temperature (arXiv: 1512.07374v2)
- [14] Michelberger P S, Champion T F M, Sprague M R, Kaczmarek K T, Barbieri M, Jin X M, England D G, Kolthammer W S, Saunders D J and Nunn J 2015 Interfacing GHz-bandwidth heralded single photons with a warm vapour Raman memory *New J. Phys.* **17** 043006
- [15] Saunders D J, Munns J H D, Champion T F M, Qiu C, Kaczmarek K T, Poem E, Ledingham P M, Walmsley I A and Nunn J 2016 A cavity-enhanced room-temperature broadband Raman memory *Phys. Rev. Lett.* **116** 090501
- [16] Happer W 1972 Optical pumping *Rev. Mod. Phys.* **44** 169–249
- [17] Molisch A F and Oehry B P 1998 *Radiation Trapping in Atomic Vapours* (Oxford: Oxford Science Publications)
- [18] Kaczmarek K T, Saunders D J, Sprague M R, Kolthammer W S, Feizpour A, Ledingham P M, Brecht B, Poem E, Walmsley I A and Nunn J 2015 Ultrahigh and persistent optical depths of cesium in kagomé-type hollow-core photonic crystal fibers *Opt. Lett.* **40** 5582–5
- [19] Rosenberry M A, Reyes J P, Tupa D and Gay T J 2007 Radiation trapping in rubidium optical pumping at low buffer-gas pressures *Phys. Rev. A* **75** 023401
- [20] Franz F A and Sooriamoorthi C E 1974 Spin relaxation within the  $6^2p_{1/2}$  and  $6^2s_{1/2}$  states of cesium measured by white-light optical pumping *Phys. Rev. A* **10** 126–40
- [21] Reim K F, Michelberger P S, Lee K C, Nunn J, Langford N K and Walmsley I A 2011 Single-photon-level quantum memory at room temperature *Phys. Rev. Lett.* **107** 053603
- [22] Lancor B and Walker T G 2010 Effects of nitrogen quenching gas on spin-exchange optical pumping of  $^3\text{He}$  *Phys. Rev. A* **82** 043417
- [23] Klein M, Xiao Y, Hohensee M, Phillips D F and Walsworth R L 2008 Stored light and eit at high optical depths (arXiv: 0812.4939)
- [24] Parniak M and Wasilewski W 2014 Direct observation of atomic diffusion in warm rubidium ensembles *Appl. Phys. B* **116** 415–21
- [25] Pitz G A, Fox C D and Perram G P 2010 Pressure broadening and shift of the cesium D2 transition by the noble gases and  $\text{N}_2$ ,  $\text{H}_2$ , HD,  $\text{D}_2$ ,  $\text{CH}_4$ ,  $\text{C}_2\text{H}_6$ ,  $\text{CF}_4$ , and  $^3\text{He}$  with comparison to the D1 transition *Phys. Rev. A* **82** 042502
- [26] Steck D A 2017 Cesium D line data <http://steck.us/alkalidata/cesiumnumbers.1.6.pdf>
- [27] McGillis D A and Krause L 1968 Inelastic collisions between excited alkali atoms and molecules. IV. sensitized fluorescence and quenching in mixtures of cesium with  $\text{N}_2$ ,  $\text{H}_2$ , HD, and  $\text{D}_2$  *Can. J. Phys.* **46** 1051–7
- [28] Nunn J 2008 Quantum memory in atomic ensembles *PhD Thesis* University of Oxford
- [29] Sangouard N, Simon C, Minar J, Afzelius M, Chaneliere T, Gisin N, Le Gouet J-L, de Riedmatten H and Tittel W 2010 Impossibility of faithfully storing single photons with the three-pulse photon echo *Phys. Rev. A* **81** 062333
- [30] Nunn J et al 2016 Theory of noise suppression in  $\lambda$ -type quantum memories by means of a cavity (arXiv: 1601.00157)
- [31] Romanov G, O'Brien C and Novikova I 2016 Suppression of the four-wave mixing amplification via Raman absorption *J. Mod. Opt.* **63** 2048–57